W-dispersion particles in repulsive potentials: Quasibound states and their lifetime

Leonid D. Shvartsman[1] and Dmitri A. Romanov[2,3,*]

[1]*The Racah Institute of Physics, The Hebrew University, Jerusalem, Israel, 91904*

[2]*Department of Physics, Temple University, Philadelphia, Pennsylvania 19122*

[3]*Center for Advanced Photonics Research, College of Science and Technology, Temple University, Philadelphia, Pennsylvania 19122*

(Received 31 August 2014; published 27 February 2015)

We consider fundamental features which emerge in the mechanics of quasiparticles with nonmonotonic (as a function of p^2) dispersion law. Quasiparticles of this kind abound in modern physics, with examples ranging from holes in quantum wells to edge magnetic states in quantum wires to photons in atomic vapors to polaritons in photonic crystals and in trapped-atom lattices. The motion of such a particle in repulsive potentials gives rise to a number of counterintuitive phenomena, which carry a promise of unusual optical manifestations. A classical particle can be trapped by repulsive potentials, and the likelihood of this trapping may increase with the value of the angular momentum. Further, in contrast to the usual quantum-mechanical notion, the particle always has a quasibound state in a two-dimensional, central-force repulsive potential, while it may have no bound states in a one-dimensional analog of this potential. The binding energy of these states and their inherent decay rate are determined by a complex interplay of the parameters of the potential, the particle dispersion law, and the value of the angular momentum. We construct the energy spectrum of quasibound states in a repulsive Coulomb potential, estimate their lifetime, and predict their optical manifestations as inverted hydrogen spectral-line series.

DOI: 10.1103/PhysRevA.91.022126 PACS number(s): 03.65.Sq, 45.20.Jj, 03.65.Ge, 03.65.Ca

I. INTRODUCTION

In modern physics and applications, a large number of charge-carrying quasiparticles appear with essentially nonquadratic dispersion, whose details can often be engineered. This abundance calls for a general investigation of new possibilities that arise when considering motion of such a particle in external potentials.

Classical mechanics, in its Hamiltonian formulation, contains the generalized coordinate, q, and generalized momentum, p, of a particle on equal footing: having started with the Hamiltonian $H(p,q)$, one is free to choose either $q(t)$ or $p(t)$ to represent the particle motion. In practical instances, however, the variable of choice is usually q, and this preference becomes overwhelming in quantum mechanics. The obvious rationale for this choice is the simple quadratic dependence of kinetic energy upon momentum, which makes it easy to exclude the momentum variable from equations of motion in the classical case and makes for a second-order partial differential equation of standard type (the Schrödinger equation) in the quantum case. On a conceptual level, this convenient quadratic dependence originates from the Galilean relativity principle [1], and its hallmark is the absence of a characteristic momentum scale.

An apparent deviation from this rule is the relativistic dispersion, which does have a characteristic momentum scale, m_0c. (This kind of dispersion is largely responsible for unusual electronic and optical properties of graphene [2–4,5]). More complex non-Galilean dispersion emerges naturally in various systems with periodic potential. In this case, the characteristic momentum scale is given by $\hbar/a$ where a is the period. For electrons in crystal lattice, the earliest example of a dynamic effect associated with such nonquadratic dispersion was probably the Bloch oscillations in strong electric fields [6]. The non-Galilean character of electron dispersion is reflected in complex shapes of the Fermi surface in metals, which determines response to external electric and magnetic fields [7] and largely influences collective effects in electron system [8]. Non-Galilean dispersion of charge carriers of various kinds can now be engineered in semiconductor heterostructures, where the characteristic momentum is given by $\hbar/L$, where L is the characteristic width of the quantum well or quantum wire. Here, the effects of non-Galilean dispersion on optical and transport properties have been explored for valence subband [9–12], conduction subbands [13–18], and also hybrid subbands [19], which carry promise of efficient terahertz emission. All these studies, however, were concerned with either free particles or particles in uniform external fields. In contrast, we investigate classical and quantum-mechanical behavior of a non-Galilean particle in a local potential and show emergence of counterintuitive localized states, which should manifest themselves optically as spectral anomalies. A simplified one-dimensional case was considered in our prior Rapid Communication [20]; here we concentrate on the role of angular momentum.

To capture alternative physics stemming from non-Galilean dispersion and be able to trace it analytically all the way to optical manifestations, we consider a particular form of well-pronounced non-Galilean dispersion, when the kinetic energy, $\varepsilon(p)$, is a nonmonotonic function of the momentum magnitude p: It initially decreases as p grows from zero to some specific $p = p_0$, and then increases with p when $p \to \infty$. (It is convenient to call particles with this type of non-Galilean dispersion W-dispersion particles, since in the one-dimensional case they have a W-shaped dispersion curve.) The energy reference point is set as $\varepsilon(0) = 0$; the function $\varepsilon(p)$ reaches at $p = p_0$ its negative minimum value $\varepsilon(p_0) = -\Delta$. The dispersion law of this kind frequently emerges in electron and/or hole subbands of quantum wells,

*daroman@temple.edu

where the values of parameters p_0 and Δ can be engineered by the well width and material composition [19]. For numerical estimates, we will refer to a particular instance of particles with exactly this dispersion law: hole subband in a realistic GaSb/AlSb quantum well of 100 Å width, where $\Delta = 6\,\mathrm{meV}$ and $p_0 = (1.82 \times 10^6) m_e\,\mathrm{g\,cm/s}$ where m_e is the electron mass [11]. This structure of the dispersion law should lead to the most pronounced dynamical consequences when the particle interacts with a repulsive potential. Indeed, in this case the values of p that lie in the positive-mass region ($p > p_0$) will correspond to a regular repulsion, while the values of p that lie in the negative-mass region ($p < p_0$) will correspond to effective attraction. In a simplified one-dimensional case, it was shown that the dynamics of such a particle exhibits a number of counterintuitive effects [20]. In particular, (1) a classical particle can penetrate under a barrier; (2) a classical particle can be trapped by a finite repulsive potential if the magnitude of this potential is smaller than Δ; and (3) a stronger, divergent potential loses the ability to trap the particle. Further, in the quantum realm, these effects are transformed into unusual patterns of scattering resonances.

In the present communication, we investigate the possibilities for a non-Galilean particle to form bound states in realistic, two-dimensional, axially symmetric repulsive potentials, including Coulomb potential. We obtain the energy spectrum and lifetime values for the bound states as depending on the characteristic parameters of both the dispersion law and the repulsive potential. In particular, we show that in this case the canonical angular momentum becomes the crucial parameter on which the very existence of bound states hinges and which determines their key characteristics. As a specific application of this general approach, we predict an anomalous optical effect in the mentioned GaSb/AlSb quantum well structures, where existence of quasibound hole-hole pairs should result in experimentally verifiable "inverted hydrogen" spectral-line series.

II. THE MODEL: CLASSICAL MECHANICS

We assume the two-dimensional dispersion law to be axially symmetric, that is, to depend only on the magnitude of the particle momentum, p. It is convenient to express the dispersion law as a function of squared variable, $\varepsilon(\mathbf{p}) = \varepsilon(p) = \tilde{\varepsilon}(p^2)$. Then, in the cylindrical coordinate system, (ρ,θ), the Hamiltonian of a free particle has the form

$$H_0(p_\rho, p_\theta, \rho) = \tilde{\varepsilon}\left(p_\rho^2 + p_\theta^2/\rho^2\right), \tag{1}$$

where p_ρ and p_θ are the canonical momenta corresponding to the coordinates ρ and θ. When the particle moves in a central-force repulsive potential $U(\rho)$ that depends only on the magnitude of the two-dimensional position vector, ρ, the Hamiltonian is augmented to $H(p_\rho, p_\theta, \rho, \theta) = U(\rho) + H_0(p_\rho, p_\theta, \rho)$. As seen in Eq. (1), in the case of a nonparabolic dispersion law, the radial and angular canonical momenta are effectively intermingled, thus preventing their separation in the usual way. Nevertheless, the coordinate θ is not present explicitly in the Hamiltonian, and this leads to the conservation of the corresponding canonical momentum, $p_\theta = M = \mathrm{const}$. This conservation law taken into account, the two-dimensional problem is reduced to a one-dimensional one, with the effective Hamiltonian:

$$H_M(p,\rho) = U(\rho) + \tilde{\varepsilon}(p^2 + M^2/\rho^2). \tag{2}$$

(From this point on, we drop the index ρ when denoting the radial canonical momentum.) Characteristically, the contribution M^2/ρ^2 is not separated in Eq. (2) in the form of a simple centripical potential, but produces instead compound $p - \rho$ terms, which are the signature of the non-Galilean nature of the particle.

To glean the essential features of the classical motion of a particle that is described by the Hamiltonian, we consider phase trajectories in the plane (ρ, p). These trajectories are determined by the equation $H_M(p,\rho) = E$; they can be classified by the value of M and the value of energy, E. As seen in Eq. (2), all phase trajectories have mirror symmetry with respect to the ρ axis. In the trivial situation of a free particle, $U(\rho) = 0$, the phase trajectories are the line(s) $p(\rho) = \pm\sqrt{\tilde{\varepsilon}_{1,2}^{-1}(E) + M^2/\rho^2}$, where $\tilde{\varepsilon}_{1,2}^{-1}(E)$ are the solutions to the equation $\tilde{\varepsilon}(z) = E$. For $E > 0$, this equation has one solution, and each energy value is represented by one phase trajectory. In the interval $-\Delta < E < 0$, there are two solutions and two phase trajectories per each energy value. Finally, $E = -\Delta$ corresponds again to one trajectory, $p(\rho) = \pm\sqrt{p_0^2 + M^2/\rho^2}$. All the trajectories approach asymptotically the straight lines $p = \pm\sqrt{\tilde{\varepsilon}_{1,2}^{-1}(E)}$ when $\rho \to \infty$, and they cross the ρ axis vertically at the points $\rho_{M,E} = M/\sqrt{\tilde{\varepsilon}_{1,2}^{-1}(E)}$. The smaller the value of M, the closer the position of this crossing point to $\rho = 0$; at $M = 0$, each trajectory degenerates into a pair of straight lines $p = \pm\sqrt{\tilde{\varepsilon}_{1,2}^{-1}(E)}$. A typical $H_M(p,\rho)$ surface and the corresponding pattern of open phase trajectories pattern are shown in Fig. 1, left panel.

When $U(\rho) \neq 0$, the topology of the described phase trajectories may change drastically, depending on the characteristics of $U(\rho)$. For the sake of simplicity, we assume the repulsive potential $U(\rho)$ to decrease monotonically as ρ grows, and $\partial U/\partial\rho$ to have no more than one extremum point. The character of the phase trajectories is determined by the number and character of the extremum points of the function $H_M(0,\rho)$. When $U(\rho) = 0$, this function has one extremum point, the minimum at $\rho_M = M/p_0$. When $U(\rho) \neq 0$, the potential pulls up the low-ρ part of the curve $H_M(0,\rho)$, and the positions of possible extremum points are determined by the equation

$$\left|\frac{\partial U}{\partial \rho}\right| + \frac{2M^2}{\rho^3}\left.\frac{\partial \tilde{\varepsilon}}{\partial z}\right|_{z=M^2/\rho^2} = 0. \tag{3}$$

Given the properties of the functions $U(z)$ and $\tilde{\varepsilon}(z)$, this equation may have up to three solutions, all lying in the negative-mass region of $\tilde{\varepsilon}(z)$ so that $\partial^2 H_M(p,\rho)/\partial^2 p$ is definitely negative at each of these points. The number of solutions that actually materialize is determined by a complex interplay of M, Δ, p_0, and the parameters of the repulsive potential: its magnitude, $U(0)$, its range being greater or smaller than ρ_M (in the case of a finite-range potential), and/or its asymptotic decrease at $\rho \to \infty$ being slower or faster than ρ^{-2} (in the case of an infinite-range potential). If all three

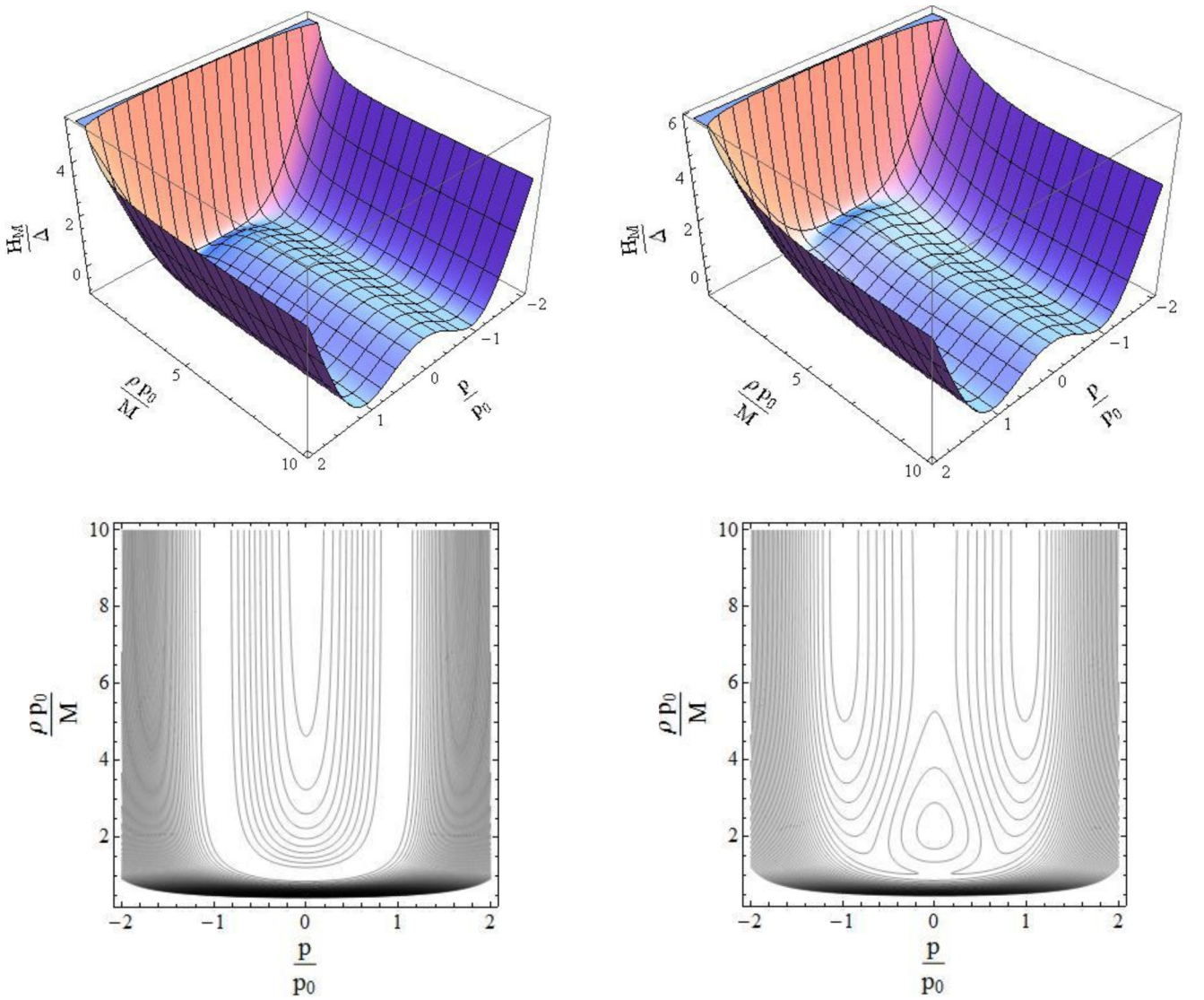

FIG. 1. (Color online) Left panel: Top: a typical surface of the effective Hamiltonian $H_M(p,\rho)$ in the case of free particle with W-shape-dispersion law. The coordinates are normalized with respect to the parameters of the dispersion law, p_0 and Δ, and the value of the angular momentum, M. Bottom: the corresponding pattern of phase trajectories. Right panel: Top: a typical $H_M(p,\rho)$ surface for a particle in an axially symmetric repulsive potential. Bottom: the corresponding pattern of phase trajectories; closed phase trajectories signify the particle localization.

extremum points exist, the first one (in the order of growing ρ) is a minimum of $H_M(0,\rho)$, the second one is a maximum, and the third one is a minimum again. Then, the first point is a saddle point of the function $H_M(p,\rho)$, the second point is a maximum, and the third point is a saddle point again. The emerging local maximum of $H_M(p,\rho)$ implies the existence of closed phase trajectories running around this maximum. Moving along such a closed trajectory, the particle is localized by a repulsive potential. The area of closed trajectories lies between the two saddle points positioned on the ρ axis. It should be emphasized that the divergence of the potential at $\rho \to 0$ per se does not preclude existence of the closed trajectories (i.e., localized states), in contrast to the situation in the one-dimensional case [20]. The physical reason for this insensitivity is that at finite M the particle is prevented from approaching the point $\rho = 0$.

The interplay of M, Δ, p_0, and the mentioned parameters of the repulsive potential generates a variety of cases of the global pattern of phase trajectories. We relegate systematic study of these cases to further publications. Here, we concentrate on the important case of repulsive Coulomb potential $U(\rho) = e^2/\rho$, where e is the effective charge, properly reduced by the polarization of the medium. As at $\rho \to \infty$ the potential decreases slower than $1/\rho^2$ and the function $H_M(0,\rho)$ is positive, Eq. (3) may have at most two solutions. If these two solutions exist, the smaller one corresponds to a saddle point of the $H_M(p,\rho)$ surface; the greater one corresponds to a maximum (at $E = E_{\max}$). The condition for these two solutions to exist can be conveniently expressed from Eq. (3) if this equation is rewritten as

$$(\partial\varepsilon/\partial z)|_{z=M/\rho} = -e^2/M. \tag{4}$$

The expression on the left-hand side is formally the velocity of a particle whose momentum is M/ρ. Thus, the prerequisite condition for the maximum to emerge is that the velocity in the negative-mass region should become greater by modulus than a given value, e^2/M. As this given value decreases to zero when M increases, the maximum necessarily emerges, provided there are sufficiently large values of the angular momentum M. [The degenerate case of one solution corresponds to an inflection point on the curve $H_M(0,\rho)$].

The phase trajectories corresponding to the two-extrema situation (i.e., to a sufficiently large M) are shown in Fig. 1, right panel. The closed trajectories exist in the energy range $0 < E < E_{\max}$, and they coexist with the open trajectories. When $E \to +0$, these closed trajectories extend to ever larger values of ρ. We would like to emphasize a counterintuitive fact: there are no classical bound states with small angular momenta, while particles with large angular momenta can be localized.

III. QUANTUM MECHANICS: QUASIBOUND STATES

In building a quantum-mechanical description, we start with the generalized Schrödinger equation, $\tilde{\varepsilon}(-\hbar^2\Delta_2)\psi + U(\rho)\psi = E\psi$, where Δ_2 is the two-dimensional Laplace operator. As with the classical motion, we use the cylindrical coordinate system, (ρ,φ); the angular momentum conservation allows us to look for the wave function in the form $\psi(\rho,\varphi) = \chi(\rho)\exp(il\varphi)$, where an integer $l = M/\hbar$ is the angular quantum number. Then, the equation for the radial wave function $\chi(\rho)$ reads

$$\tilde{\varepsilon}\left[-\hbar^2\left(\frac{\partial^2}{\partial\rho^2} + \frac{1}{\rho}\frac{\partial}{\partial\rho}\right) + \frac{\hbar^2 l^2}{\rho^2}\right]\chi + U(\rho)\chi = E\chi. \quad (5)$$

Note that due to nonparabolicity in Eq. (5) the ρ derivatives act on the term $\hbar^2 l^2/\rho^2$ as well as on the wave function, thus producing complicated cross terms with higher powers of ρ in their denominators. To build a semiclassical approximation, we substitute in Eq. (5) the wave function in the form $\chi(\rho) = (\rho)^{-1/2}\exp[iS(\rho)/\hbar]$, look for the action function $S(\rho)$ in the series form $S(\rho) = S_0(\rho) + \hbar S_1(\rho) + \cdots$, and solve iteratively for $S_0(\rho)$ and $S_1(\rho)$. After some tedious algebra, the radial wave function is obtained as $\chi_E^{(1,2)}(\rho) = A[\Omega_E^{(1,2)}(\rho)]^{-1/2}\exp[(i/\hbar)\int\Theta_E^{(1,2)}(\rho)d\rho]$, where

$$\begin{aligned}\Theta_E^{(1,2)}(\rho) &= \sqrt{\tilde{\varepsilon}_{1,2}^{-1}[E - U(\rho)] - \frac{M^2}{\rho^2}};\\ \Omega_E^{(1,2)}(\rho) &= \rho\Theta_E^{(1,2)}(\rho)\left.\frac{\partial\tilde{\varepsilon}(z)}{\partial z}\right|_{z=[\Theta_E^{(1,2)}(\rho)]^2+\frac{M^2}{\rho^2}},\end{aligned} \quad (6)$$

and A is the normalizing constant. Here, the solutions marked by the indices 1 and 2 correspond to the two isoenergetic classical trajectories which coexist in the region $-\Delta < E - U(\rho) < 0$.

Now, we apply these general results to a particular case of the Coulomb potential. To obtain analytic results, we model the nonmonotonic dispersion law as $\tilde{\varepsilon}(p^2) = -p^2/(2m) + \beta(p^2)^2$. Here, parameter m quantifies the negative-mass behavior at small p, and the physical meaning of parameter β is that it determines the relative depth of the side minimum of the dispersion law: $\beta = \Delta/p_0^4$. (In the mentioned particular case of GaSb/AlSb quantum well, $m \approx 0.117m_e$ and $\beta = (9.6\times10^{-10})m_e^{-3}\ \mathrm{s}^2/\mathrm{g}^3\,\mathrm{cm}^2$). Then, the characteristic constants that determine the position of the minimum point are $p_0^2 = (4m\beta)^{-1}$, $\Delta = (16m^2\beta)^{-1}$ and the inverse function in Eq. (6) is given by the simple formula, $\tilde{\varepsilon}_{1,2}^{-1}(z) = p_0^2(1 \pm \sqrt{z/\Delta + 1})$. It is convenient to use the characteristic length, $\rho_0 = e^2/\Delta = 16\beta m^2 e^2$, whose physical meaning is the distance at which the Coulomb energy is equal to the characteristic energy of the dispersion law. Using the dimensionless variable, $x = \rho/\rho_0$, the functions in Eq. (6) are obtained as

$$\begin{aligned}\Theta_E^{(1,2)}(x) &= p_0\rho_0\sqrt{1 \pm \sqrt{1 + \frac{E}{\Delta} - \frac{1}{x}} - \frac{c^2}{x^2}},\\ \Omega_E^{(1,2)}(x) &= \frac{4e^2}{p_0}x\Theta_E^{(1,2)}(x)\left(\pm\sqrt{1 + \frac{E}{\Delta} - \frac{1}{x}}\right),\end{aligned} \quad (7)$$

where the angular momentum M is represented by a dimensionless constant, $c^2 = M^2/(p_0^2\rho_0^2) = M^2\Delta^2/(p_0^2e^4)$. Zeros of $\Omega_E^{(1,2)}(x)$ determine the turning points of the quasiclassical motion. As seen in Eq. (7), these turning points are of two kinds: (i) zeros of the function $\Theta_E^{(1,2)}(x)$ that correspond to the regular quasiclassical turning points, and (ii) the irregular turning point, $x_b = \Delta/(\Delta + E)$, which emerges due to the nonmonotonic form of the dispersion law. The respective positions of these regular and irregular turning points on the x axis determine qualitatively the quasiclassical behavior of the particle. We consider only the situation of a large angular momentum, i.e., $c \gg 1$. In this case, the regular turning points of both the closed trajectory and the open trajectory lie at $x \sim c$, that is, far to the right from the irregular turning point. The closed trajectory corresponds to $\Theta_E^{(2)}(x)$ in Eq. (7); it has two turning points, $x_l^{(2)}$ and $x_r^{(2)}$. The expression under the square root behaves linearly in x near both of the turning points. Consequently, the usual Bohr-Sommerfeld quantization formula for the discrete energy spectrum is valid; and it gives

$$\int_{x_l^{(2)}}^{x_r^{(2)}} dx\,\Theta_{E_n}^{(2)}(x) = \pi\hbar(n + 1/2)$$

where n is a natural number. In particular, when $x_l^{(2)}, x_r^{(2)} \ll x_b$, the quantized energy levels are determined by the algebraic equation,

$$\frac{1}{\sqrt{1 + E_n/\Delta}\sqrt{\sqrt{1 + E_n/\Delta} - 1}} - 4c = \frac{4\hbar}{p_0\rho_0}\left(n + \frac{1}{2}\right). \quad (8)$$

The condition $c \gg 1$ implies $E_n \ll \Delta$; in this case, the approximate solution to Eq. (8) is easily obtained as

$$E_n = \tilde{E}(n + l + 1/2)^{-2}, \quad (9)$$

where the energy scale is $\tilde{E} = p_0^2e^4/(8\hbar^2\Delta) = me^4/(2\hbar^2)$. For the mentioned example of GaSb/AlSb quantum well, taking for estimates an averaged value of the dielectric constant $\varepsilon \approx 14$, the characteristic energy scale is estimated as $\tilde{E} = 8$ meV for the hole localization in external potential and $\tilde{E} = 4$ meV for hole-hole interaction. As $\Delta = 6$ meV, the use of Eq. (9) is

completely justified only for nonzero values of l, especially in the first of these two cases. As expected, these energy levels form the inverse hydrogen series, which correspond to quantization of a negative-mass particle localized in the repulsive Coulomb potential. Note that the restriction $E_n \ll \Delta$ implies $l^2 \gg me^4/(2\hbar^2\Delta)$.

The obtained quantum states are quasistationary, because the particle can tunnel to the isoenergetic open trajectory. This tunneling occurs mainly in the vicinity of the saddle point of the $H_M(p,\rho)$ surface, i.e., near the turning point $x_l^{(2)}$. However, peculiarities of this tunneling process allow the localized states to exist for a considerably long time. Indeed, the tunneling implies alteration of the trajectory type $\Theta_{E_n}^{(2)}(x)$ to $\Theta_{E_n}^{(1)}(x)$. To achieve this alteration, it is not enough for the particle to just penetrate through the under-barrier intertrajectory distance. The particle has to reach the remote branching point of the function $\Theta_{E_n}(x)$ [the function whose two branches are $\Theta_{E_n}^{(2)}(x)$ and $\Theta_{E_n}^{(1)}(x)$] in the complex plane of the variable z. According to Eq. (7), the position of this branching point is determined by the condition $1 + E/\Delta - 1/x = 0$; i.e., this is the would-be irregular turning point x_b that is moved very far in the under-barrier region. According to this scenario, the lifetime of a localized quantum state, $\tau_n \propto \hbar(dE_n/dn)^{-1}\exp(\Phi_n)$, is determined by the exponent

$$\Phi_n = -i\frac{p_0\rho_0}{\hbar}\left(\int_{x_l^{(2)}}^{x^{(1)}} dx\,\Theta_{E_n}^{(2)}(x) + \int_{x^{(1)}}^{x_b} dx\left(\Theta_{E_n}^{(2)}(x) - \Theta_{E_n}^{(1)}(x)\right)\right). \tag{10}$$

(Here, $x^{(1)}$ is the single turning point of the open trajectory.) Using the fact that at small values of x the behavior of the functions $\Theta_{E_n}^{(2)}(x)$ and $\Theta_{E_n}^{(1)}(x)$ is mainly determined by the term c/x^2 under the square root in Eq. (7), we obtain from Eq. (10) a rough estimate of the exponent Φ_n as

$$\Phi_n \approx (p_0\rho_0 c/\hbar)\left[\ln\left(x_l^{(2)}/x^{(1)}\right) + (1/2)(1+E_n/\Delta)^{1/4}\right] \approx (p_0\rho_0 c/\hbar)[\ln(4\sqrt{2}c) + 1/2]. \tag{11}$$

At large values of c (that is, of l), Φ_n grows large and thus allows for considerably long lifetimes of the localized states. These localized states can be characterized by a dimensionless figure of merit, constructed as the product of the lifetime of the $n = 0$ state, τ_0, and the energy distance between this state and the next one, $E_0 - E_1$:

$$\kappa = \tau_0(E_0 - E_1)/\hbar \propto e^{l/2}(4\Delta/\tilde{E})^{l/2}(l)^l. \tag{12}$$

The steep dependence on l in Eq. (12) ensures that the localized states with large l will exist long enough to be physically relevant. The comparison of Eqs. (9) and (12) shows also that there is a trade-off between the energy distances in the quasidiscrete spectrum and the lifetimes of the corresponding localized states: the larger l, the longer the localized states exist but the smaller the distance between their energy levels.

IV. CONCLUSIONS

In conclusion, we have shown that the classical and quantum mechanics of non-Galilean particles are rich in unusual phenomena. We have described the properties of counterintuitive two-dimensional quasistationary quantum states, localized in a repulsive Coulomb potential only with sufficiently large values of angular momentum. Model energy spectrum and lifetimes of these states have been calculated analytically. The most obvious optical manifestation of these states should be unusual "inverted hydrogen" spectral-line series in hole-type quantum wells, with the characteristic energy scale in the single-meV range. These series would be the signature of quasibound hole-hole pairs (charged bosons), whose possible existence has been discussed recently [11,12]. In a broader sense, trapping of *W*-dispersion quasiparticles by repulsive potentials may result in experimentally observable effects in all the diverse systems mentioned in the Introduction. Moreover, as dispersion-law engineering extends to systems with inherently nonquadratic dispersion such as magnetoexcitons in quantum-Hall situation [21–24], photons in atomic vapors [25,26], or in photonic crystals [27] and polaritons in trapped-atom systems [28], analogs of counterintuitive particle trapping may be expected in those systems as well.

ACKNOWLEDGMENT

The authors gratefully acknowledge financial support from Yissum, the Technology Transfer Company of the Hebrew University.

[1] L. D. Landau and E. M. Lifshitz, *Mechanics*, 3rd ed. (Pergamon, Oxford, 1976).

[2] K. S. Novoselov, A. K. Geim, S. V. Morozov, D. Jiang, Y. Zhang, S. V. Dubonos, I. V. Grigorieva, and A. A. Firsov, Electric field effect in atomically thin carbon films, Science **306**, 666 (2004).

[3] K. S. Novoselov, A. K. Geim, S. V. Morozov, D. Jiang, M. I. Katsnelson, I. V. Grigorieva, S. V. Dubonos, and A. A. Firsov, Two-dimensional gas of massless Dirac fermions in graphene, Nature **438**, 197 (2005).

[4] A. K. Geim and K. S. Novoselov, The rise of graphene, Nat. Mater. **6**, 183 (2007).

[5] M. I. Katsnelson, K. S. Novoselov, and A. K. Geim, Chiral tunnelling and the Klein paradox in graphene, Nat. Phys. **2**, 620 (2006).

[6] L. Esaki and R. Tsu, Superlattice and Negative Differential Conductivity in Semiconductors, IBM J. Res. Develop. **14**, 61 (1970).

[7] I. M. Lifshitz, M. Y. Azbel, and M. I. Kaganov, *Electron Theory of Metals* (Consultants Bureau, New York, 1973).

[8] D. L. Maslov, V. I. Yudson, and A. V. Chubukov, Resistivity of a non-galilean-invariant fermi liquid near pomeranchuk quantum criticality, Phys. Rev. Lett. **106**, 106403 (2011).

[9] A. V. Chaplik and L. D. Shvartsman, Kinetic phenomena in the quantum-sized layers of hole semiconductors, Sov. Phys. Surf. Phys. Chem. Mech. **2**, 73 (1982).

[10] R. K. Hayden, D. K. Maude, L. Eaves, E. C. Valadares, M. Henini, F. W. Sheard, O. H. Hughes, J. C. Portal, and L. Cury, Probing the hole dispersion curves of a quantum well using resonant magnetotunneling spectroscopy, Phys. Rev. Lett. **66**, 1749 (1991).

[11] L. D. Shvartsman and D. A. Romanov, in *Physics of Semiconductors: 27th International Conference on the Physics of Semiconductors*, edited by J. Menendes and C. G. Van de Walle (American Institute of Physics, Melville, 2005).

[12] L. D. Shvartsman and J. E. Golub, in *Bose Einstein Condensation*, edited by A. Griffin, D. W. Snoke, and S. Stringari (Cambridge University Press, New York, 1994).

[13] D. A. Romanov and L. D. Shvartsman, Weak-field magnetoconductance oscillations caused by magnetic surface levels (MSL), Solid State Commun. **53**, 677 (1985).

[14] B. Y. Gu, W. D. Sheng, and J. Wang, Oscillatory magnetoconductance in quantum waveguides with lateral multi-barrier structures, Int. J. Mod. Phys. B **12**, 653 (1998).

[15] E. B. Gorokhov, D. A. Romanov, S. A. Studenikin, V. A. Tkachenko, and O. A. Tkachenko, The effect of a nonmonotonic potential profile on edge magnetic states, Semiconductors **32**, 970 (1998).

[16] J. R. Shi and B. Y. Gu, Magnetoconductance oscillations of two parallel quantum wires coupled through a potential barrier, Phys. Rev. B **55**, 9941 (1997).

[17] S. V. Korepov and M. A. Liberman, Transport properties of double quantum wires in a magnetic field, Phys. Rev. B **60**, 13770 (1999).

[18] Z. Y. Zeng, Y. Xiang, and L. D. Zhang, Ballistic electronic transport in quantum cables, J. Appl. Phys. **88**, 2617 (2000).

[19] S. de-Leon, L. D. Shvartsman, and B. Laikhtman, Band structure of coupled InAs/GaSb quantum wells, Phys. Rev. B **60**, 1861 (1999).

[20] L. D. Shvartsman, D. A. Romanov, and J. E. Golub, Mechanics of particles with nonmonotonic dispersion laws, Phys. Rev. A **50**, R1969 (1994).

[21] C. Kallin and B. I. Halperin, Excitations from a filled landau-level in the two-dimensional electron-gas, Phys. Rev. B **30**, 5655 (1984).

[22] A. Pinczuk, J. P. Valladares, D. Heiman, L. N. Pfeiffer, and K. W. West, Light-scattering determination of roton densities of states in 2-dimensional landau-level excitations, Surf. Sci. **229**, 384 (1990).

[23] S. R. E. Yang and G. C. Aers, Magnetorotons in quasi-one-dimensional electron-systems in the absence of kohn theorem, Phys. Rev. B **46**, 12456 (1992).

[24] M. Kang, A. Pinczuk, B. S. Dennis, L. N. Pfeiffer, and K. W. West, Observation of multiple magnetorotons in the fractional quantum hall effect, Phys. Rev. Lett. **86**, 2637 (2001).

[25] L. V. Hau, S. E. Harris, Z. Dutton, and C. H. Behroozi, Light speed reduction to 17 metres per second in an ultracold atomic gas, Nature **397**, 594 (1999).

[26] M. M. Kash, V. A. Sautenkov, A. S. Zibrov, L. Hollberg, G. R. Welch, M. D. Lukin, Y. Rostovtsev, E. S. Fry, and M. O. Scully, Ultraslow group velocity and enhanced nonlinear optical effects in a coherently driven hot atomic gas, Phys. Rev. Lett. **82**, 5229 (1999).

[27] J. D. Joannopoulos, S. G. Johnson, J. N. Winn, and R. D. Meade, *Photonic Crystals: Molding the Flow of Light*, 2nd ed. (Princeton University Press, Princeton, NJ, 2008).

[28] H. Zoubi, Collective interactions in an array of atoms coupled to a nanophotonic waveguide, Phys. Rev. A **89**, 043831 (2014).